CFD analysis and application of dynamic mode decomposition for resonant-mode identification and damping in an SGT-100 DLE combustion system

A. Abou-Taouk[1*], S. Sadasivuni[2], D. Lörstad[3], G. Bulat[2], L. E. Eriksson[1]

[1] Chalmers University of Technology, Hörsalsvägen 7A, SE-41296 Gothenburg, Sweden
[2] Siemens Industrial Turbomachinery Ltd PO Box 1, Waterside South, Lincoln, LN5 7FD, UK
[3] Siemens Industrial Turbomachinery AB, SE-612 83 Finspong, Sweden

Abstract

This paper presents result of a turbulent reacting flow simulation based on a hybrid Unsteady Reynolds Averaged Navier Stokes /Large Eddy Simulation model (Menter's SAS-SST model) applied to an experimental version of an industrial gas turbine combustion chamber at a pressure of 6 bar. The kinetics were represented by a recently developed in-house 4-step reaction mechanism using 7 species. A reasonably good agreement with measurements is found concerning velocity, temperature, pressure loss, mixture fraction and fuel mass fraction. The dynamic mode decomposition algorithm is also used here in order to identify some resonant modes and to quantify their respective frequency and damping. A number of low frequency modes with combustion dynamics included are observed and compared with the measurements.

Introduction

Combustion is a multi-disciplinary field involving areas such as chemical kinetics, fluid dynamics and thermodynamics. In real life, most industrial gas turbine combustors are difficult to study due to complex geometries and multiple inlets, fast chemistry, dilution with burnt gases and high pressures. In addition to this, the flow is often turbulent and therefore the combustion reactions occur within a wide range of eddy scales which characterize the turbulence. This implies that robust and accurate models for combustion chemistry and its interaction with turbulence are needed for the design and development of future gas turbine combustors. In order to obtain accurate and validated models one also needs experimental data which is difficult to obtain since these devices often operate at high pressure. The rapid increase in computer power in recent years has made reacting flow simulations feasible using more sophisticated models such as hybrid Unsteady Reynolds Averaged Navier Stokes /Large Eddy Simulation model (URANS/LES) and LES, which resolves the large scales and flow-flame interactions, and the uncertainty of the combustion modelling is then narrowed to the unresolved sub-grid scale motions. LES of reacting flow is under intense development and investigated in numerous studies [1–11]. Viewed from industrial design perspective CFD-analysis using LES is still often too expensive in terms of computer power, mesh resolution, simulation time and therefore using a hybrid RANS/LES model can be an advantage for the industry. Scale Adaptive Simulation (SAS) [12] is an example of this type of model which switches to an LES mode in unsteady flow if the resolution of the grid is sufficient and to an URANS mode close to the walls. Several studies on combustion have been using the SAS-model [12–15].

Reacting flows are dominated by different mechanisms (fluid dynamics, kinetics, interfaces, and structures) which exhibit instabilities. A significant challenge in the development and operation of gas turbines is to prevent different combustion instabilities by predicting their dominating frequencies. In a premixed confined flame the acoustic waves produced by combustion might reflect on the boundaries and propagates back into the flame zone. Due to recirculation zones in a swirling flow, the information could propagate upstream by convection but also by acoustic waves [2]. The flame itself is sensitive to waves and may feed energy into the oscillations and thus cause an amplification of one or several resonance modes. The lean premixed swirled combustion burners are therefore prone to instabilities, which can cause structural damages due to large amplitude vibrations and/or high thermal loads at walls. Flame flashback and blow off of the flame can also be obtained from the instabilities [16]. There exist numerous methods of predicting such instabilities, where the DMD algorithm [17] is a recently developed method which enables to extract aero-acoustic modes from a data set recorded using CFD or experiments.

To evaluate the DMD approach together with the SAS-SST turbulence model and a global reaction mechanism, a reference multi-point injection and premixed burner (SGT-100 DLE [18–20]) is simulated and the results are compared with experiments.

Background and challenges

In this work the numerical simulations are conducted using the SAS-SST model which is based on the two-equation SST model. This model blends between a $k-\epsilon$ and a $k-\omega$ formulation for the turbulence closure. In the SAS model, the von Karman length scale is added within the turbulence length scale equation, so that the model changes dynamically from a URANS to LES resolution mode. This means that no explicit grid information is required, but still the model is able to partially resolve the turbulent spectrum [12]. The majority of the published combustion articles on gas turbine burners based on the hybrid URANS/LES and LES are tested at atmospheric pressure and are for relatively simple geometrical configurations.

The work described in this paper aims to validate the SAS-SST model together with the M4 [13] global reaction mechanism for the experimental version of SGT-100 industrial gas turbine combustor which is designed and manufactured at Siemens Industrial Turbomachinery Ltd, UK. The combustor was studied experimentally in the high pressure rig at German Aerospace Center (DLR) Stuttgart, Germany, [18–20]. The burner geometry has been studied previously with RANS (Reynolds Averaged Navier Stokes) [13], hybrid RANS/ LES [13], scalar dissipation rate model [21] and LES [8–11]. All these simulations were performed at the operating pressure of 3 bar. In this work, an operating pressure of 6 bar is used and considered to be a greater challenge due to generation of higher unsteady pressure amplitudes. However, the operating conditions (pressure and

*Corresponding author: abdallah@chalmers.se

temperature) studied and discussed both in this paper and in the experiment are different from the real SGT-100 gas turbine condition.

In the DLR test rig, the burner is fitted to a square combustion chamber with quartz windows, as shown in Figure 1. The air is supplied through the circumferential inlet around the swirler and inside of which the natural gas [18] is injected at various injector location in the swirl generator (36 holes) [8–11, 13, 18–21]. The flow is turned through the swirler vanes into the prechamber, where the air and fuel mixture exits into the sudden expansion square combustion chamber. One-dimensional Raman for scalar and PIV velocity measurements profiles are available at four streamwise locations x/R = 2.42; 2.87; 3.33 and 4.00, where R is the prechamber radius shown in Figure 1.

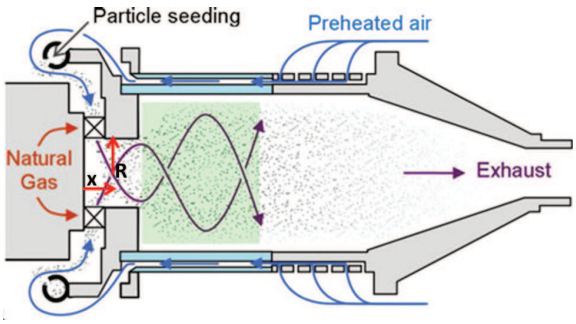

Figure 1: Experimental setup.

Reaction rate calculation

The combined turbulence-chemistry interaction model, that is the Eddy Dissipation Model (EDM) - Finite Rate Chemistry (FRC), in Ansys CFX [22], is chosen for the URANS/LES CFD analysis. This model is valid for several reactions that range from low to high Damköhler numbers. The advantage of this model is that the reaction rates can be limited by turbulent mixing in some regions of the domain and limited by kinetics in other areas in the domain. The FRC model computes the reaction rate based on the following expression:

$$\dot{\omega}_i = A_i \prod_{j \in \mathcal{A}_i} \left(\frac{\rho Y_j}{W_j} \right)^{\mu_{j,i}} T^{B_i} \exp\left(-E_{a_i}/(\mathcal{R}T)\right) , \quad (1)$$

where $\mathcal{A}_i$ is the ensemble of species involved in reaction i, ρ denotes the density, $\mathcal{R}$ denotes the universal gas constant, W_j is the molecular weight of species j, B_i is the temperature exponent, E_{ai} is the activation energy, A_i is the pre-exponential factor and $\mu_{j,i}$ is the reaction orders of species j in reaction i. The FRC model computes one reaction rate for each individual reaction used in the global reaction mechanism. In the EDM model the reaction rate of reaction i is computed as:

$$\dot{\omega}_i = A_i \frac{\epsilon}{k} \prod_{j \in \mathcal{A}_i} min\left(\frac{[I]}{\mu'_{j,i}} \right) , \quad (2)$$

where $\frac{\epsilon}{k}$ is the turbulent mixing rate and $[I]$ is the molar concentration of component I. The EDM model computes one reaction rate respectively for each reaction in the global reaction mechanism. The EDM-FRC model thus selects the minimum rate from the two models.

The kinetics is modeled by a recently developed in-house 4-step (Table 1) reaction mechanism (M4) [13]. The M4 global mechanism is composed of four reactions: (i) the fuel oxidation into CO and H_2; (ii) H_2 and O_2 into H_2O; (iii) CO and O_2 into CO_2; and (iv) the water gas shift reaction, CO and H_2O into CO_2 and H_2. Jones and Lindstedt [23] have previously published (around 30 years ago) a 4-step reaction mechanism that is similar to the M4 mechanism. A deeper discussion about the differences can be found in the article by Abou-Taouk et al. [13]. The reaction rates in the M4 mechanism are expressed following equation 1.

Reaction	A_i	B_i	E_{a_i}	Reaction order
$CH_4 + \frac{1}{2} O_2 \rightarrow CO + 2H_2$	1.4E+12	0.8	36.5	$[CH_4]^{0.7}$, $[O_2]^{0.97}$
$H_2 + \frac{1}{2} O_2 \leftrightarrow H_2$	5.309E+17	-1.48	40.0	$[H_2]^{0.55}$, $[O_2]^{1.01}$
$CO + \frac{1}{2} O_2 \leftrightarrow CO_2$	2.333E+13	-0.4	35.5	$[CO]^1$, $[O_2]^{0.5}$
$CO + H_2O \leftrightarrow CO_2 + H_2$	2.836E+13	0.4	32.857	$[CO]^1$, $[H_2O]^1$

Table 1: Kinetic rate data (unit in cm, s, kcal and mol) for an operating pressure of 6 bar.

The M4 mechanism [13] is developed using well-established optimization tools, where the coefficients of the 4-step global methane/air chemistry are determined from a set of reference detailed chemistry solutions.

Numerical simulation

The CFD-domain is shown in Figure 2. Specified mass flow rates are imposed at the inlet boundaries for the main air inlet, the burner panel inlet and the 36 fuel inlets. The cooling air inlet and the exhaust pipe leakage are excluded in the CFD-simulation. The preheated air temperature is set to 685 K at the air inlets and 320 K for the fuel inlets. The outlet boundary condition is set to 6 bar and a no-slip adiabatic condition is imposed on all walls. The global equivalence ratio in the burner is approximately 0.6.

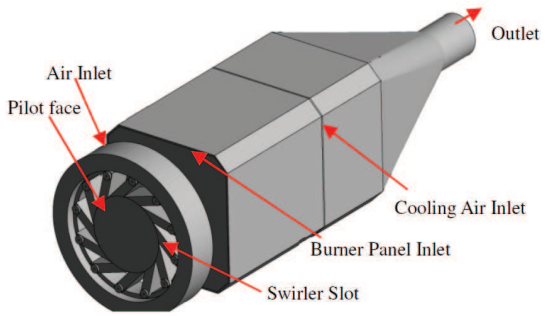

Figure 2: CFD-domain of combustor.

Reynolds Averaged Navier Stokes equations are solved along with the energy and species mass fractions. ANSYS CFX [22] software is used which is based on the finite volume method. The software uses a coupled solver and the solution approach uses a fully implicit discretization of the equations at any given time step. The high resolution scheme (which is a bounded second-order upwind biased discretization) was applied for discretization in space and time. The mesh is composed of 11 million hexahedral cells and has the same resolution as in previous work [8–11, 13, 21] with the difference that the exhaust can is included in this work. The statistics are first converged for a non-reactive case, and the flow is then advanced in time with

combustion for about 100 ms (seven flow-through times) until the flame is well established and statistics are accumulated for another 100 ms. The time step for the simulation was set to 2.5e-5 s, which implies an averaged CFL number of 3. The total CPU time needed for the simulation was approximately 40000 hours. The flame is anchored on the pilot face, while the main flame is located in the combustion chamber and takes the shape of a hollow cone. This burner is operated in premixed mode, however, the equivalence ratio close to the central axis is below the ignition limit and reaches a slightly rich level near the shear layer. The flame topology consists of regions of corrugated flame fronts due to the high turbulence levels in this shear layer. According to the experimental measurements by Stopper et al. [20] the Damköhler numbers of Da∼1.4-2.5 and Karlovitz numbers of Ka∼77-230 are obtained for these flames. The obtained Damköhler and Karlovitz numbers for this operating point corresponds to a regime where thickened flame fronts and local extinctions are to be expected according to the regime diagrams by Borghi [24]. The total pressure drop across the combustor is approximately 2.6% of the combustor mean pressure of 6 bar, which is in acceptable agreement with the experimentally measured pressure drop of the order of 3% across the combustor [19].

Figure 3 and Figure 4 present a comparison of PIV measured data [20] and simulated streamwise/spanwise mean velocities at four different locations shown in Figure 7. The CFD results agree well with the measured main flow field. The outer recirculation zone is well captured at all positions, however the inner recirculation zone is not fully reproduced at third and fourth location. From phase-correlated mean velocity values in the experiment performed by Stopper et al. [20] it is observed that the axial velocity at center axis (inner recirculation zone) for the axial coordinate x=18.6 mm is fluctuating substantially, the variation is between -30 m/s to -10 m/s. At this location the CFD predicts a mean-averaged axial velocity of -20 m/s. The inner recirculation variation in velocity is explained by a periodic vortex shedding by Stopper et al. [20]. The same conclusion can also be drawn looking at the streamlines and results from the DMD algorithm below.

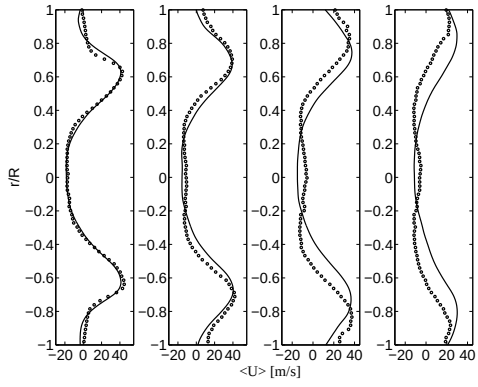

Figure 3: Streamwise averaged velocity at four different locations shown in Figure 7. Symbol: Experiments [20]. Solid-line: CFD.

Figure 5 shows a comparison between an instantaneous axial velocity snapshot from CFD and phase-correlated mean flow field experimental data in the form of streamlines. It can be observed that the inner shear layer consists of small vortices which are created and dissipate rapidly. The vortex field visible

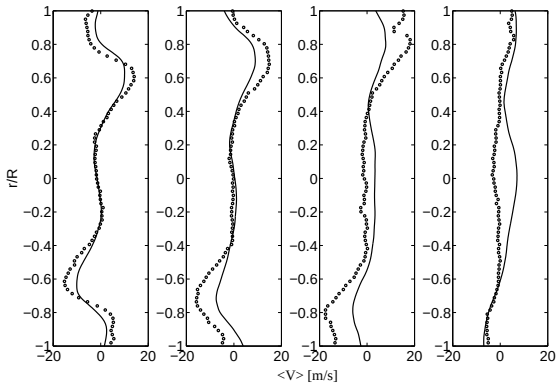

Figure 4: Spanwise averaged velocity at four different locations shown in Figure 7. Symbol: Experiments [20]. Solid-line: CFD.

in the instantaneous flow field is not steady, but rather is observed to move back and forward. From the instantaneous CFD results one can observe that the vortices visible in Figure 5 display an oscillation cycle. Different vortices are created close to the prechamber wall, move downstream with the flow and often merge together while dissipating.

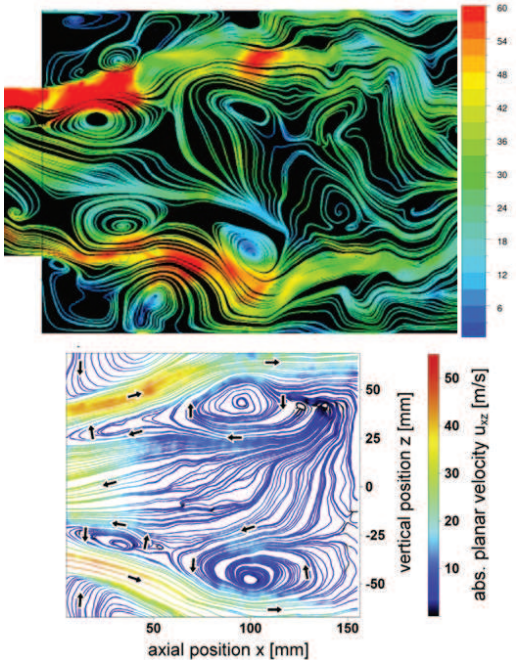

Figure 5: Streamline plots of an instantaneous snapshot from CFD (top) and a phase-correlated mean flow field at phase intervals 6 (bottom) coming from the experiment [20].

Figure 6 shows a comparison of simulated axial velocity in the present work (top) and from the simulation performed earlier [13]. The later simulation was performed at an operating pressure of 3 bar where the exhaust pipe was excluded. The velocity levels are generally similar. Some differences can be seen close to the central axis. In order to capture main features, such as temperatures, velocities and major species it seems that the exhaust pipe nay bot be needed. However, the CFD without an exhaust pipe in the present simulation has difficulties to capture the low resonant modes measured in the experiment [20].

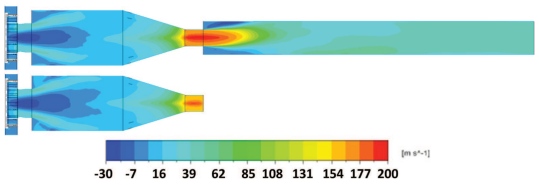

Figure 6: Contour plot of mean axial velocity [m/s] at an operating pressure of 6 bar (top) and 3 bar (bottom) [13].

The contour plots in Figure 7 (a cut along the central x-y plane though the flame) show a comparison between the predicted CFD mean temperature and the ensemble averaged temperature values measured by Raman spectroscopy [20]. The plot from the CFD and experiments are shown untill the radial coordinate corresponding to y = 47.5 mm due to measurements restriction (the combustor wall is located at y = 82.5 mm). In the experimental data a small temperature peak is visible at y∼24 mm, x∼18.7. This temperature peak is not predicted by the CFD simulation. However, Stopper et al. [20] describes this hot spot as likely to be an artifact from the raw data analysis due to that the temperature reference value is switched from cold unburned gas to completely reacted gas at adiabatic flame temperature at this position.

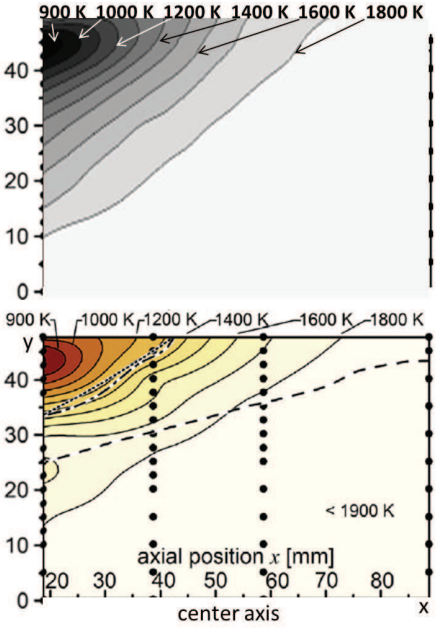

Figure 7: Contour plots of the mean temperature between the CFD results (top) and the experimental data [20] (bottom). The dots show the four different locations used for comparison in this work.

Figure 8 presents a comparison of PIV measured data [20] and simulated mean temperature at four different locations shown in Figure 7. The temperature has been normalized by the maximum temperature. The CFD results agree well with the measured mean temperature. Some small deviations can be observed around r/R=0.6. This area corresponds to the inflow region of the fuel air mixing stream.

In order to reduce emissions it is important to obtain a well premixed flame. The mixing process depends on different design parameters, residence time (volume) and turbulence intensity. However, the thermoacoustic oscillations are likely to increase in premixed flames which need to be controlled either by active or passive ways. A good measure of mixing process is to plot the mixture fraction and fuel fraction. Figure 9 shows radial profiles of the mean mixture fraction from the CFD predictions displayed with the experimental results [20] at four different locations shown in Figure 7. From the phase-correlated experimental data in [20] it is clear that a large variation of the mixture fraction is measured at the first location (x=18.6 mm) in the radial region corresponding to 25mm $<$ r $<$ 50 mm. This area corresponds to the same inflow region mentioned before. The predicted result by CFD seems to be slightly underpredicting the mean mixture fraction in the inner recirculation zone. One of the reasons behind the variations in mixture fraction and consequently the equivalence ratio may be due to the pressure variations in the combustion chamber [16] and also might be due to URANS mode in these regions which makes difficult to capture the mixing process compared to LES.

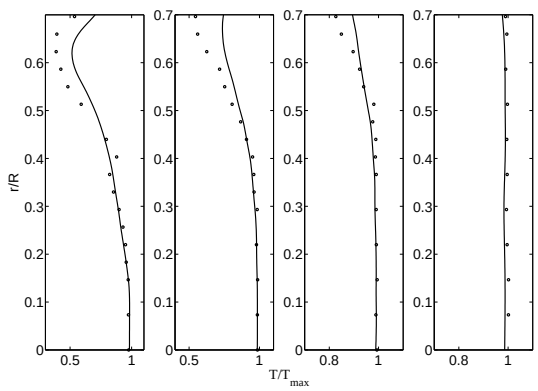

Figure 8: Mean normalized temperature at different locations shown in Figure 7. Symbol: Experiments [20]. Solid-line: CFD.

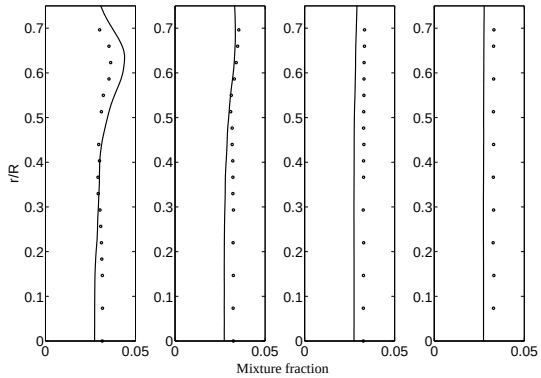

Figure 9: Mean mixture fraction at different locations shown in Figure 7. Symbol: Experiments [20]. Solid-line: CFD.

Results from the DMD method

The DMD technique is applied here to identify the resonant modes in the burner, to extract the mode structures and to quantify the respective damping modes. A part of the DMD method is to apply single value decomposition in the whole domain. The modes that are identified by the DMD technique are

associated with a fixed oscillation frequency and growth/decay rate, determined by DMD without requiring knowledge of the governing equations. This is in contrast to methods, such as the POD, which produce a set of modes without the associated temporal information. The DMD method is based on a data set recorded using CFD or experiments. The data is recorded over a fixed time interval which contains information from both the linear and the nonlinear structures of the domain. One of the advantages of the DMD method is based on the freedom of the selection of 2-dimensional planes in the computational domain. The physical variables chosen in the planes at each snapshot can also be varied leading to a significant reduction of CPU time for the post processing.

Previously published results using CFD and experiment [8, 13] show that the combustion chamber features a small ($\sim$ 20 mbar) periodic pressure amplitude at an operating pressure of 3 bar. However, at an operating pressure of 6 bar used in this work, the pressure amplitude is increased (113 mbar in the experiment). This oscillation was observed in the experiment [8] at the frequency 220 Hz with the variations $\pm$ 19 Hz. The CFD predicted a pressure amplitude of 100 mbar without any excitation of the flow field. This can be an advantage since the results of the DMD can be sensitive to how the flow field is disturbed [25]. The Strouhal number (St) is a dimensionless number describing oscillating flow mechanisms. The Strouhal number is given as $St = \frac{fL}{U}$ where f is the frequency of vortex shedding, L is a chosen characteristic length and U is a characteristic velocity of the fluid. The Strouhal number from the CFD was calculated to 0.2 based on the $f = 220Hz$, L is the prechamber diameter and U is the average inlet velocity of the burner. This value indicates that the pressure fluctuation at 220 Hz is associated with the flow field. An FFT analysis of the CFD-results show three distinct low-frequency peaks at $\sim$90 Hz, $\sim$180 Hz and $\sim$220 Hz. In the present DMD simulation, the sampling time interval between two snapshots was selected such that a pressure fluctuation/oscillation at high frequency, e.g. 1000 Hz could be predicted. The time step in the CFD simulations was chosen to 25 μs and a snapshot is recorded every five time steps. The recording time is also important since it determines the lowest possible frequency that can be predicted. The DMD is performed with 400 snapshots, corresponding to the lowest detectable frequency of 20 Hz (the inverse of the recorded time is roughly equal to the lowest frequency). Figure 10 shows the obtained frequencies and the respective damping coefficients using the DMD technique. The plot is based on 400 snapshots, where the DMD analysis was based on temperature, axial velocity and pressure at five different planes, as shown in Figure 11. A smaller (more negative) damping coefficient indicates larger damping. All of the predicted coefficients are negative, which means that the amplitude will be decreased (damped out). In Figure 10 the three lowest frequencies (88, 190, 226 Hz) agrees well with the FFT analysis (90, 180, 220 Hz). However, the experiment measured the lowest frequency equal to 220 Hz.

Figure 11 and Figure 12 show normalized axial velocity at different planes with a phase-shift corresponding to approximately 20°. The plots are extracted from the DMD algorithm for the mode with the frequency corresponding to 226Hz. A circumferential rotating mode can be observed from these two figures. The transient data suggest that vortices are created close to the prechamber wall and form a periodic vortex shedding which downstream in the burner displays merging and dissipation.

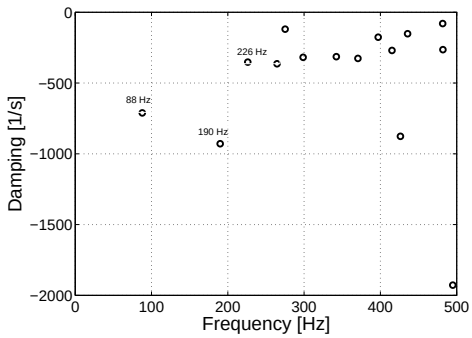

Figure 10: DMD modes

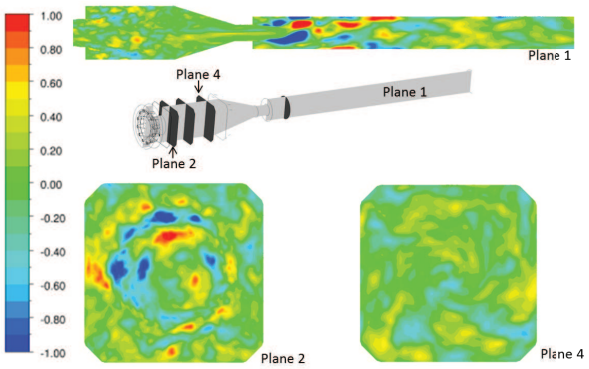

Figure 11: DMD mode at f=226Hz showing the normalized axial velocity at three different planes at time t1.

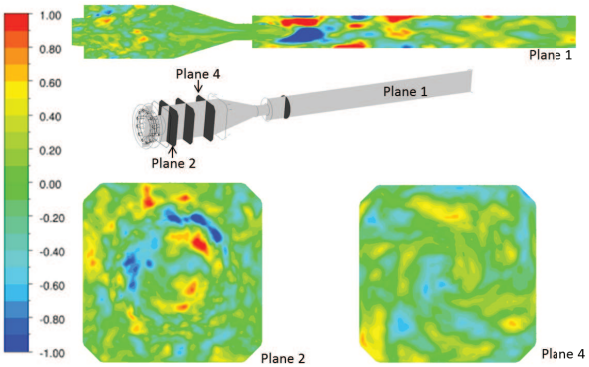

Figure 12: DMD mode at f=226Hz showing the normalized axial velocity at three different planes at time t2.

Conclusion

The aim of this paper was to investigate a 4-step global reaction mechanism together with the SAS-SST turbulence model for natural gas using the laboratory version of the Siemens SGT-100 DLE industrial gas turbine combustor. The simulation was conduct for the operating pressure of 6 bar. Flame properties along with statistical data agree well with the measurements. More specifically, velocity profiles, flame temperatures, pressure loss, fuel mole fraction and mixture fraction profiles compares well with the experimental data. A number of low frequency combustion modes were identified with the DMD algorithm, proposed by Schmidt [17]. One of these modes were obtained at a frequency of 226 Hz and compares well with the thermo-acoustic oscillation mode obtained in the experiment

[20] at the frequency of 220 Hz.

Acknowledgements

This work was funded by the Swedish Energy Agency, Siemens Industrial Turbomachinery AB, GKN Aerospace Engine Systems Sweden, and the Royal Institute of Technology through the Swedish research program TURBO POWER. The authors also would like to acknowledge Siemens Industrial Turbomachinery Ltd, Lincoln, UK, for their permission to use the Turchemi test case and to publish this paper.

References

[1] Boudier. G., Gicquel. L. Y. M., Poinsot. T. J. *Combust. Flame*, 155(1-2):196–214, 2008.

[2] Franzelli. B., Riber. E., Gicquel L. Y., Poinsot. T. *Combust. Flame*, 159(2):621–637, 2012.

[3] Fiorina. B., Vicquelin. R., Auzillon. P., Darabiha. N., Gicquel. O., Veynante. D. *Combust. Flame*, 157:465–475, 2010.

[4] Subramanian. V., Domingo. P., Vervisch. L. *Combust. Flame*, 157(3):579–601, 2010.

[5] Moureau. V., Domingo. P., Vervisch. L. *Combust. Flame*, 158(7):1340–1357, 2011.

[6] Cavallo-Marincola. F., Ma. T., Kempf. A. M. *Proc. Combust. Inst.*, 34(1):1307–1315, 2013.

[7] Duwig. C., Nogenmyr. K. J., Chan. C., Dunn. M. J. *Combust. Theory and Modelling*, 15:537–568, 2011.

[8] Bulat. G., Jones. W.P., Marquis. A.J. *Proc. Combust. Inst.*, 34(2):3155–3164, 2013.

[9] Bulat. G., Jones. W. P., Marquis. A. J. *Combust. Flame*, 161(7):1804–1825, 2014.

[10] Bulat. G., Fedina. E., Fureby. C., Meier. W., Stopper. U. *Proc. Combust. Inst.*, 35(3):3175–3183, 2015.

[11] Bulat. G., Jones. W. P., Navarro-Martinez. S. Large eddy simulations of isothermal confined swirling flow in an industrial gas-turbine. *International Journal of Heat and Fluid Flow*, In Press, Corrected Proof, Available online 24 November 2014.

[12] Egorov. Y., Menter. F. R. Development and Application of SST-SAS Turbulence Model in the DESIDER Project. In *Second Symposium on Hybrid RANS-LES Methods*, Corfu, Greece, 2007.

[13] Abou-Taouk. A., Sadasivuni. S., Lörstad. D., Eriksson. L.-E. Evaluation of global mechanisms for LES analysis of SGT-100 DLE combustion system. In *ASME Turbo Expo 2013, June 3-7, 2013, San Antonio, Texas, USA,(GT2013-95454)*, 2013.

[14] Abou-Taouk. A., Sigfrid. I., Ronald. W., Eriksson. L.-E. A four-step global reaction mechanism for CFD simulations of flexi-fuel burner for gas turbines. In *Turbulence, Heat and Mass Transfer 7*, volume 7, pages 785–788, 2012.

[15] Rebosio. F. B. Methods for the Numerical Simulation of Combustion Instabilities. *PhD thesis*, 2012.

[16] Lieuwen. T. C., Yang. V. Combustion instabilities in gas turbine engines. *Progress in Astronautics and Aeronautics American Institute of Aeronautics and Astronautics, Inc.*, 2005.

[17] Schmidt. P. J. *Journal of Fluid Mechanics*, 656:5–28, 2010.

[18] Stopper. U., Aigner. M., Meier. W., Sadanandan. R., Stöhr. M., Kim. I. *J. Eng. Gas Turbines Power*, 131(2):021504-1–021504-8, 2009.

[19] Stopper. U., Aigner. M., Ax. H., Meier. W., Sadanandan. R., Stöhr. M., Bonaldo. A. *Exp. Thermal and Fluid Science*, 34(3):396–403, 2010.

[20] Stopper. U., Meier. W., Sadanandan. R., Stöhr. M., Aigner. M., Bulat. G. *Combust. Flame*, 160(10):2103–2118, 2013.

[21] Sadasivuni. S. K., Bulat. G., Sanderson. V., Swaminathan. N. Numerical application of scalar dissipation rate combustion model to Siemens DLE combustors. *Proceedings of ASME Turbo Expo*, GT2012–68483, 2012.

[22] http://www.ansys.com/default.asp, 2013.

[23] Jones. W. P., Lindstedt. R. P. *Combust. Flame*, 73:233–249, 1988.

[24] Borghi. R. Recent Advances in Aerospace Sciences. *in: C. Casci, C. Bruno (Eds.)*, Plenum Press, New York, 1985, pp. 117–138.

[25] Larusson. R., Andersson. N., Eriksson. L.E. Investigation of a Separated Nozzle Flow with Transonic Resonance Using Dynamic Mode Decomposition. *Chalmers Research Report 2014:04*, ISSN 1652-8549, 2014.